Chemical Engineering Journal 454 (2023) 140126

Contents lists available at ScienceDirect

Chemical Engineering Journal

journal homepage: www.elsevier.com/locate/cej

Review

Insights into reactive species generation and organics selective degradation in Fe-based heterogeneous Fenton-like systems: A critical review

Ling Li [a,1], Zhuo Yin [b,1], Min Cheng [a], Lei Qin [a], Shiyu Liu [a], Huan Yi [a], Mingming Zhang [a], Yukui Fu [a], Xiaofeng Yang [a], Xuerong Zhou [a], Guangming Zeng [a,*], Cui Lai [a,*]

[a] College of Environmental Science and Engineering and Key Laboratory of Environmental Biology and Pollution Control (Ministry of Education), Hunan University, Changsha 410082, PR China
[b] Department of Urology, Second Xiangya Hospital, Central South University, Changsha 410011, PR China

ARTICLE INFO

Keywords:
Fe catalysts
H_2O_2 activation
Surface active sites
Reactive species
Selective oxidation

ABSTRACT

Currently, iron (Fe)-based heterogeneous Fenton-like processes have been widely employed for treating organic pollutants in wastewater. During such processes, organic pollutants are usually attacked by the generated reactive species and thus decomposed into some intermediates, further CO_2 and H_2O. Therefore, a comprehensive understanding of reactive species generation and utilization is significant for achieving the selective and effective degradation of organic pollutants in complicated water matrix. Herein, on the basis of the comprehensive literature survey, this review briefly analyzes the H_2O_2 activation mechanism over surface active sites of Fe catalysts, including surface Fe sites, oxygen vacancies, and electron distribution-polarized micro-areas, from the points of reactive species generation. Meanwhile, the guidelines for improving the Fenton-like performance of Fe catalysts are proposed based on this information. Furthermore, the selective oxidation of organic pollutants by generated reactive species, including high-valent iron oxo species (Fe(IV) = O/Fe(V) = O), hydroxyl radical (•OH), superoxide radical ($\bullet O_2^-$), and singlet oxygen ($^1O_2$) are discussed with emphasis on the existing form and chemical characteristics of reactive species. Finally, the existing challenges and the prospects for water treatment are proposed from mechanism research and practical application aspects. We hope this review can provide a deeper understanding of the fundamentals of Fe-based heterogeneous Fenton-like reaction, and help readers to select a suitable Fenton-like system for practical applications.

1. Introduction

Recently, the inevitable industrialization and urbanization have made environmental pollution a global challenge that damages ecosystems and endangers life.

Therefore, it is of highly importance to develop environmental remediation technologies to eliminate contaminants. Fenton process, which consists of reactive species production via activating hydrogen peroxide (H_2O_2) through the electron cycle involving Fe^{2+}/Fe^{3+}, has been widely employed for destructing refractory organic pollutant in wastewater [1–3]. Thereinto, heterogeneous Fenton-like reactions catalyzed by Fe catalysts have drawn increasing notice for broad application because Fe is the second most abundant metal in nature and almost non-toxic. Moreover, Fe catalysts can efficiently activate H_2O_2 to generate reactive species in a wide pH range [4–6].

In the past few decades, numerous Fe catalysts, roughly including natural Fe catalysts that exist in natural environment (i.e., Fe-containing clay, Fe-containing zeolite, Fe oxide minerals, and Fe sulfide minerals) [7–10], and synthetic Fe catalysts (i.e., Fe-containing metal organic frameworks (MOFs), loaded Fe catalysts, Fe-containing resins, Fe-containing complex, zero-valent Fe, Fe-containing perovskite, Fe oxychloride (FeOCl) and single-atom Fe catalysts) [11–19] have been developed to study their catalytic behavior in heterogeneous Fenton-like system, and the development history since 1990 are concluded in Fig. 1.

During such catalytic processes, the surface Fe sites are usually considered as the main active sites for H_2O_2 activation [17,20–22]. Recently, relevant studies also reported that some microstructures over Fe catalysts surface, such as oxygen vacancies (OVs), and electron distribution-polarized micro-areas have also been regarded as potential active sites for activating H_2O_2 [23–26]. The routes of H_2O_2

---

* Corresponding authors.
E-mail addresses: zgming@hnu.edu.cn (G. Zeng), laicui@hnu.edu.cn (C. Lai).
[1] These authors contribute equally to this article.

https://doi.org/10.1016/j.cej.2022.140126
Received 27 August 2022; Received in revised form 13 October 2022; Accepted 28 October 2022

Fig. 1. The development of Fe catalysts in Fenton-like process.

decomposition at these active sites can be primarily described as adsorption, electron transfer, and cleavage of O—O bond, Fe-O bond, or O—H bond, following by generation of corresponding reactive species such as high-valent iron oxo species (i.e., Fe(IV) = O and Fe(V) = O), hydroxyl radical (•OH), superoxide radical ($\bullet O_2^-$), and singlet oxygen ($^1O_2$) [27–29]. Nevertheless, conflicting views on H_2O_2 activation and reactive species generation still exist. For instance, some studies have pointed out a changeover of reactive species from •OH to Fe(IV) = O with pH transitioning from acidic to near-neutral in Fe^0/H_2O_2 system [30,31], however this was refuted by other studies that excluded the function of Fe(IV) = O in Fe^0/H_2O_2 system [32,33]. Likewise, Chen et al. found that both •OH and a weak oxidant (possibly Fe(IV) = O) were produced in the ferrihydrite-induced Fenton-like reaction [34], differing from other studies that focused mainly on the presence of •OH in the ferrihydrite/H_2O_2 system [35,36]. Therefore, it remains important and desirable to understand the generation of reactive species in Fe-based Fenton-like reactions, where the key is the H_2O_2 activation mechanism over active sites.

In addition to reactive species generation, there is ongoing controversy regarding the selective degradation of organic pollutants by reactive species. In the majority of literature relating to Fe-based Fenton-like reactions, it is considered that •OH is non-selective [29], $\bullet O_2^-$ and other non-radical species involving $^1O_2$ and Fe(IV) = O/Fe(V) = O are able to selectively degrade organic pollutants owing to the nature of these reactive species [37–39]. For example, $\bullet O_2^-$ has been reported to react actively with some electrophilic compounds such as carbon tetrachloride (CCl_4) owing to its strong nucleophilicity [40,41]. Meanwhile, the electrophilic Fe(IV) = O and $^1O_2$ prefer reacting with electron-rich pollutants in the manner of adding to the unsaturated bonds like S=O, C=C, and/or electron transfer [42]. Conversely, •OH is generally accepted to show universal reactivity with most target pollutants. Nevertheless, Chen et al. proposed that in Fe-oxidized carbon nanotubes (OCNT)/H_2O_2 system with surface-localized •OH as the dominant radical, the organic pollutants (i.e., methyl blue (MB) and chrysoidine G (CG)) showing high affinity to catalyst could be degraded with higher rate constants than the organic pollutants (i.e., 4-chlorophenol (4-CP) and atrazine (ATZ)) showing low affinity to catalyst [43]. That is to say, except for the nature of reactive species, their existing form (i.e., surface-bound or free) is also a key factor for achieving selective oxidation.

Recently, numerous reviews have systematically discussed the types of Fe catalysts in heterogeneous Fenton-like reactions, the characterization techniques for identifying Fe catalysts, as well as the modification strategies for enhancing Fenton-like activity of Fe catalysts [4,44–48]. There are also reviews that discussed the interfacial mechanisms of Fe-based heterogeneous Fenton-like reactions including homogeneous catalysis mechanism, heterogeneous catalysis mechanism, and heterogeneous reaction-induced homogeneous mechanism [29,49]. In addition, the application of Fe-based heterogeneous Fenton-like reactions for degrading emerging pollutants, and important factors influencing the Fenton-like performance of Fe catalysts have also been summarized [5,6,50]. These reviews made great progress in summarizing Fe-based heterogeneous Fenton-like reactions and promoted their application. Nevertheless, to our knowledge, there is no comprehensive review analyzing the mechanism of H_2O_2 decomposing into reactive species over active sites, and elucidating the mechanism of selective degradation of organic pollutants. Herein, in this critical review, the interactions between H_2O_2 and surface active sites of Fe catalysts, including surface Fe sites, oxygen vacancies, and electron distribution-polarized micro-areas were scrutinized in-detail from the aspect of reactive species generation. Meanwhile, the selective oxidations of organic pollutants were discussed with special attention to the existing form and chemical characteristics of generated reactive species. The

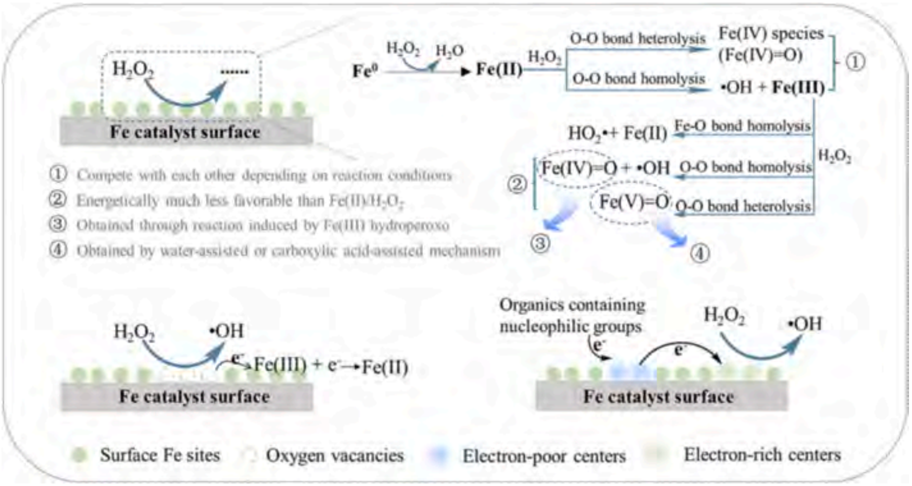

Fig. 2. The decomposition behavior of H_2O_2 at surface Fe sites, oxygen vacancies, and electron distribution-polarized micro-area.

existing challenges and suggestions for further research were also put forward, which intended to provide useful information on the development of Fe-based heterogeneous Fenton-like systems for environmental application.

2. The activation mechanism of H_2O_2 over surface active sites on Fe catalysts

Fe-based heterogeneous Fenton-like reactions have been commonly employed to treat organic pollutants in wastewater, which show great potential and prosperous application for in-situ destruction of toxic and recalcitrant organic pollutants. Although the basic knowledge for such Fenton-like processes have been excavated, there are still different views on the activation mechanism of H_2O_2. In-depth understanding the interaction between H_2O_2 and surface active sites is paramount for explaining the activation mechanism, which may provide theoretical guidance for regulating the generation of reactive species. The typical surface active sites and reactive species in natural Fe catalysts-based heterogeneous Fenton-like systems have been summarized in Table S1, and that of synthetic Fe catalysts have been summarized in Table S2. On the basis of information in Table S1 and Table S2, the main catalytic active sites for H_2O_2 activation could be regarded as surface Fe sites, oxygen vacancies, and electron distribution-polarized micro-areas (Fig. 2).

2.1. Surface Fe sites

Since the discovery of heterogeneous Fenton-like reaction, surface Fe sites have been considered as the typical active sites for activating H_2O_2 because of the significant function of Fe in classical homogeneous Fenton process [29]. As present in Table S1 and Table S2, surface Fe sites mainly exist in the valence state of zero-valence (Fe^0), divalence (Fe(II)), and trivalence (Fe(III)) to react with H_2O_2, then causing production of various reactive species.

2.1.1. Zero-valent Fe

Over the past decades, Fe^0 has attracted significant attention as surface active sites during Fenton-like reactions because of the low redox potential of Fe(II)/Fe^0 (−0.44 V) [65]. In general, Fe^0 does not directly activate H_2O_2 to generate reactive species, but serve as the source of Fe(II) and H_2O_2. For example, the dissolved oxygen (DO) in solution can accept two electrons from Fe^0 to produce H_2O_2 (Eq. (1)), and Fe^0 could be quickly oxidized to Fe(II) through two-electrons transfer process with H_2O_2 (Eq. (2)) [51,52]. Du et al. prepared microscale zero-valent iron (mZVI) for Fenton-like degrading sulfamethoxazole. The results indicated that Fe^0 was firstly oxidized to Fe(II) through two-electron transfer reaction, the generated Fe(II) then activated H_2O_2 to form •OH to degrade sulfamethoxazole [51]. Likewise, Yang et al. proposed that the process of Fe^0 oxidation by DO was spontaneous and could lead to the Fe(II) generation, which then together with H_2O_2 to initiate reactive species generation [53].

$$Fe^0 + O_2 + 2H^+ \rightarrow Fe(II) + H_2O_2 \tag{1}$$

$$Fe^0 + H_2O_2 + 2H^+ \rightarrow Fe(II) + 2H_2O \tag{2}$$

Nevertheless, the reaction rates of Fe^0 with H_2O_2/DO are highly pH-dependent. As previous literature reported, neutral and alkaline conditions (i.e., pH = 5) usually favored the precipitation of more iron hydroxides/oxides, which could cover Fe^0 and hinder the contact of Fe^0 with H_2O_2/DO, thus deteriorating the reaction rate [52,54]. While lowering the pH to extremely acidic conditions (i.e., pH = 1) could lead to rapid dissolution of Fe and therefore low utilization of Fe^0, which may also diminish the catalytic performance [53].

Except for reaction rates, the reactive species types formed in Fe^0/H_2O_2/DO system may also vary with solution pH [31,33,55]. In a typical process, the production of reactive species in Fe^0/H_2O_2/DO system is generally arrived from the Fe(II)/H_2O_2 reaction, where pH variation usually drive the mechanism changeover from •OH under acidic condition (i.e., pH = 3) to Fe(IV) = O under circumneutral pH (i.e., pH = 5 and 7). The influencing mechanism will be discussed in the section of divalent Fe. Therefore, the hypothesis that Fe(IV) = O was mainly existed under circumneutral pH in Fe^0/H_2O_2/DO system was proposed by some researchers. For example, according to the quenching efficiency of 2-propanol under different pH, Katsoyiannis et al. concluded that the reaction between Fe^0 and H_2O_2/DO generated •OH at pH 3, and a more selective reactive species (likely Fe(IV) = O) was generated at circumneutral pH [31]. Sedlak et al. also studied the variation of reactive species at different pH in Fe^0/H_2O_2/DO system based on the results of probe compounds oxidation. To be specific, the oxidation of benzonic acid and 2-propanol that could only be oxidized by •OH decreased as pH increasing from 3 to 7. While the oxidation products yields of ethanol and methanol that could react with both •OH and Fe(IV) = O increased until pH 7. These demonstrated that •OH was the main oxidant at acidic condition, while at higher pH, a different oxidant (i.e., Fe(IV) = O) was mainly presented [30,55].

However, this statement proposed according to the yields of probes oxidation products, that reactive species can be changed from •OH at acidic pH to Fe(IV) = O at near-neutral pH, was questioned by Pang et al. [32,33]. They believed that the different yields of oxidation products at various pH may be related to the complex reactions of •OH with the compound. To be specific, •OH generally reacted with probe compound to produce some reactive organic radical intermediates prior to form stable products. The solution chemistry (i.e., absence or presence of iron redox species) at different pH may interfere with the further conversion of these organic radical intermediates into corresponding products through reacting with these reactive organic radical intermediates [32,56], therefore leading to the distinct yields of products. They also used methyl phenyl sulfoxide (PMSO) and dimethyl sulfoxide (DMSO) as indicators to confirm the presence of Fe(IV) species since a specific oxygen-atom transfer tended to happen between these compounds and Fe(IV) = O, and resulting in the generation of corresponding sulfones (methyl phenyl sulfone ($PMSO_2$) as well as dimethyl sulfone ($DMSO_2$)). The results indicated that no sulfone products were observed at pH range of 2–9, which ruled out the function of Fe(IV) in Fe^0/H_2O_2/DO system [33]. This contradictory result may be related to the following reasons: (i) there is no Fe(IV) = O presented in Fe^0/H_2O_2/DO system. Nevertheless, the oxidation of pollutants may occur mainly on/or near the Fe^0 surface at circumneutral pH, and under acidic conditions, it may occur mainly in aqueous solution. Hence, the quenching agent such as 2-propanol presented in aqueous solution would have different effect on the removal efficiency at acidic pH and circumneutral pH. It was thus misapprehensive that a different active species such as Fe(IV) = O was generated [57]; (ii) the insufficient use of PMSO and DMSO may result in the lack of $PMSO_2$ and $DMSO_2$ production due to the interference from •OH, since previous studies reported that PMSO and DMSO could also react with •OH in a faster reaction rate ($k_{\bullet OH,\ DMSO} = 7.00 \times 10^9\ M^{-1}\ s^{-1}$, $k_{\bullet OH,\ PMSO} = 3.61 \times 10^9\ M^{-1}\ s^{-1}$) [58,59] than with Fe(IV) ($k_{Fe(IV),\ DMSO} = 1.26 \times 10^5\ M^{-1}\ s^{-1}$, $k_{Fe(IV),\ PMSO} = 1.23 \times 10^5\ M^{-1}\ s^{-1}$) [60].

2.1.2. Divalent Fe

The reaction between H_2O_2 and Fe(II) has been extensively researched since the discovery of their oxidative ability by H.J.H. Fenton [29]. Even so, it is still controversial whether the active species in such reaction process is •OH resulting from O—O bond homolysis (Eq. (3)) or ferryl species (i.e., Fe(IV) = O) arising from O—O bond heterolysis (Eq. (4)) within Fe(II)–H_2O_2 complex [28,29,61]. These two pathways are usually in competition depending on the conditions (i.e., solution pH and the chemical environment of Fe) [63]. As mentioned above, the variation of solution pH may lead to mechanism changeover from •OH to Fe(IV) = O in Fe(II)/H_2O_2 reaction, and this may be related to the effect of pH on the coordination environment around Fe [63–65]. For instance, the OH^- might compete with H_2O_2 to coordinate with catalyst

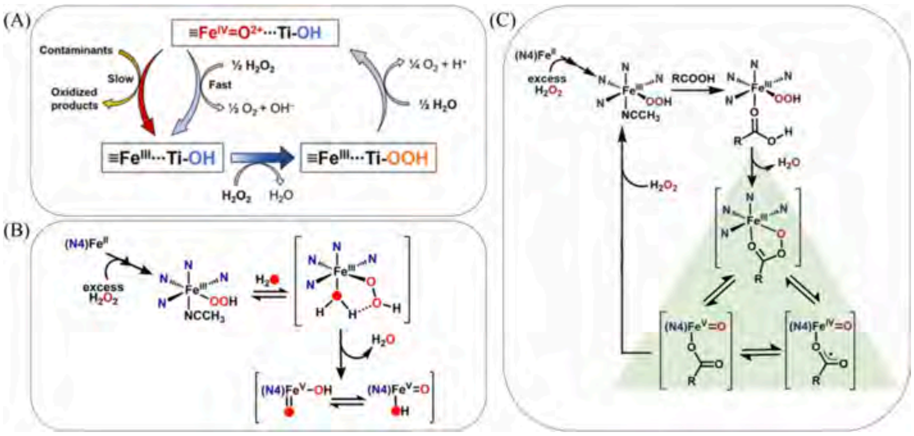

Fig. 4. (A) Proposed reaction pathway in FeTi-ox/H_2O_2 system [77]; (B) Scheme for the water-assisted mechanism and (C) carboxylic-acid-assisted mechanism [83].

oxidative reactivity between these two reagents observed in experiments [76]. In fact, in most of Fe-based Fenton-like reactions, the reaction between H_2O_2 and Fe(III) is usually underappreciated because of its relatively lower reaction rate. The primary proposed role of Fe(III) is acting as a source of Fe(II), and this process is often considered as the rate-limiting process in Fenton-like reactions [79,80]. It is attractive to understand more roles of Fe(III) in the process of H_2O_2 activation to promote the development of Fe-based Fenton-like reactions.

For example, except for O—O bond homolysis, some studies also proposed interesting reactions induced by Fe(III) hydroperoxo to generate Fe(IV) = O [77,81]. To be specific, Kim et al. found that in FeTi-ox/H_2O_2 system, the Fe(III)-Ti-OH over catalyst surface tended to react with H_2O_2 and form a stable Fe(III)-Ti-OOH complex. Then Fe(III)-Ti-OOH complex could react with water and result in the generation of Fe(IV) = O^{2+} (Fig. 4(A)). The strong interaction between H_2O_2 and TiO_2 support was considered to be an important factor triggering this process [77]. This finding provides a new insight into the role of support in Fe catalysts. In fact, except for allowing better dispersion of Fe sites on the catalysts surface, it is also proposed that the support may strongly react with H_2O_2 to form a stable complex [67]. Then affecting the reaction between H_2O_2 and Fe on the catalysts surface, and thus the identity and reactivity of consequent reactive species.

Recently, Waite et al. also proposed a mechanism of Fe(IV) = O generation from Fe(III) hydroperoxo in homogeneous $[Fe^{III}(OH)(tpena)]^+$/H_2O_2 system. They reported that $[Fe^{III}(OH)(tpena)]^+$ could react with H_2O_2 to form $[Fe^{III}(OOH)(tpena)]^+$ complex (Eq. (7)). The $[Fe^{III}(OOH)(tpena)]^+$ could then decompose to $[Fe^{IV}(O)(tpena)]^+$ and •OH via O—O bond homolysis with rate constant of 0.29 s^{-1} (Eq. (8)). Meanwhile, the combination of $[Fe^{III}(OOH)(tpena)]^+$ and $[Fe^{III}(OH)(tpena)]^+$ also led to the generation of $[Fe^{IV}(O)(tpena)]^+$ with rate constant to be 2.0×10^5 $M^{-1}s^{-1}$. Besides, quantification of these reactive species showed that $[Fe^{IV}(O)(tpena)]^+$ was generated in much higher yields than •OH. All of these data indicated that the reaction between $[Fe^{III}(OOH)(tpena)]^+$ and $[Fe^{III}(OH)(tpena)]^+$, rather than homolysis of O—O bond of $[Fe^{III}(OOH)(tpena)]^+$ mainly contributed to the formation of $[Fe^{IV}(O)(tpena)]^+$. They also found that at higher H_2O_2 concentration, $[Fe^{III}(OOH)(tpena)]^+$ could further react with H_2O_2 ($k = 1.5 \times 10^2$ $M^{-1}s^{-1}$) and lead to the generation of more •OH, which provided more guidance for investigating the mechanism of Fe(III)/H_2O_2 reaction [81].

$$Fe(III) + H_2O_2 \rightarrow Fe(II) + HO_2\cdot + H^+ \tag{5}$$

$$HO_2\cdot \rightleftharpoons \cdot O_2^- + H^+ \tag{6}$$

$$[Fe^{III}(OH)(tpena)]^+ + H_2O_2 \rightarrow [Fe^{III}(OOH)(tpena)]^+ + H_2O \tag{7}$$

$$[Fe^{III}(OOH)(tpena)]^+ + H_2O \rightarrow [Fe^{IV}(O)(tpena)]^+ + \cdot OH + H_2O \tag{8}$$

For the generation of Fe(V) = O species, the water-assisted and carboxylic acid-assisted mechanisms have been proposed during the process of hydrocarbon oxidations [82–84], and a number of Fe(N4) complexes with *cis*-labile sites have been reported to follow these mechanisms. For example, the $[Fe^{II}(TPA)(NCCH_3)_2]^{2+}$ (TPA = tris(2-pyridylmethyl)-amine) in acetonitrile could react with excess H_2O_2 and generate (TPA)Fe(III)(OOH) intermediate. Then water molecule could bind to distal oxygen atom of (TPA)Fe(III)(OOH) intermediate through hydrogen-bonding, leading to heterolysis of O—O bond and loss of terminal OH as water, finally forming an FeV(O)(OH) oxidant (Fig. 4(B)) [83,84]. Like water, it is also found that in the mixture of acetic acid and acetonitrile, carboxylic acid could bind to the Fe center and assist in the generation of FeV(O) through promoting the O—O bond cleavage within Fe(III) hydroperoxo (Fig. 4(C)) [83,85]. Although these mechanisms are rarely reported in Fe-based heterogeneous Fenton-like reactions, the above findings undoubtedly provide new insights into the regulation of Fe(IV) = O/Fe(V) = O production in Fe-based heterogeneous Fenton-like reactions.

In short, surface Fe sites (Fe^0, Fe(II), and Fe(III)) can effectively activate H_2O_2 to produce various reactive species including Fe(IV) = O/Fe(V) = O, •OH, and •O_2^-. Additionally, great attention should be paid to the factors such as reaction environment (i.e., pH and solvent) and electronic structure of Fe center, since these may influence the H_2O_2 decomposition behavior, and therefore the generation of reactive species during Fenton-like reactions. Also, the operating factors such as dosage of Fe catalysts and H_2O_2 may affect the types of reactive species, because the generated reactive species will react with excess Fe catalysts (Eqs. 9–11) and H_2O_2 (Eqs. 12–14) [6,47], therefore leading to the conversion or vanishing of reactive species.

$$Fe(III) + HO_2\cdot \rightarrow Fe(II) + O_2 + H^+ \tag{9}$$

$$Fe(III) + \cdot O_2^- \rightarrow Fe(II) + O_2 \tag{10}$$

$$Fe(II) + \cdot OH \rightarrow Fe(III) + OH^- \tag{11}$$

$$H_2O_2 + \cdot OH \rightarrow HO_2\cdot + H_2O \tag{12}$$

$$H_2O_2 + HO_2\cdot \rightarrow O_2 + H_2O + \cdot OH \tag{13}$$

$$H_2O_2 + \cdot O_2^- \rightarrow O_2 + OH^- + \cdot OH \tag{14}$$

2.2. *Oxygen vacancies*

OVs are generally considered as the most prevalent anion defects on metal oxides, where the neighboring electrons that previously occupied

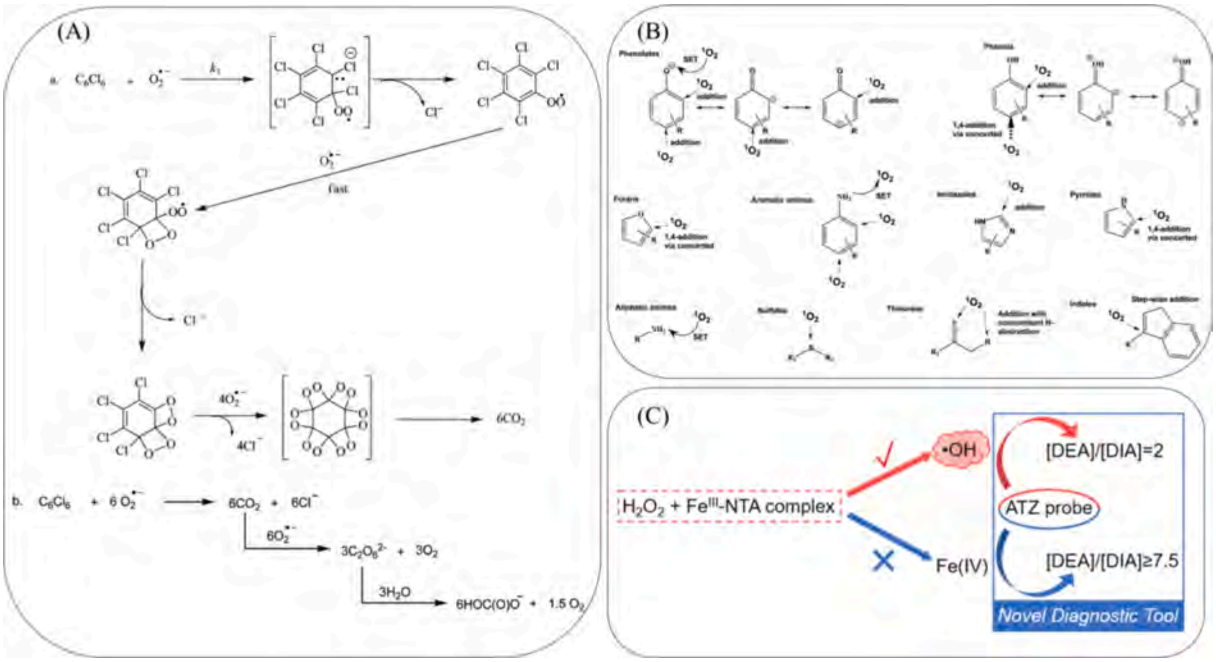

Fig. 9. (A) The possible reaction mechanism between C_6Cl_6 and $\bullet O_2^-$ [41]; (B) Major reaction mechanisms of $^1O_2$ with structurally diverse organic compounds [39]; and (C) Schematic illustration of the mechanism to distinguish Fe(IV) from •OH by determining the molar radio of DEA to DIA [131].

3.2. Selective oxidation based on the chemical characteristics of reactive species

3.2.1. $\bullet O_2^-$ and $^1O_2$

$\bullet O_2^-$ and its conjugate acid $HO_2\bullet$ ($HO_2\bullet \rightleftharpoons \bullet O_2^- + H^+$, $pK_a = 4.88$) (Eq. (6)), are another types of radicals commonly detected in Fe-based Fenton-like systems, which can be generated through the interaction between Fe(III) and H_2O_2 (Eq. (5)), or interaction between •OH and H_2O_2 (Eq. (12)). Most of previous researches have reported that $\bullet O_2^-$ is a versatile reactant with strong nucleophilicity, which can react with organic pollutants by one-electron transfer, proton abstraction, or nucleophilic substitution (Fig. 7) [106,113]. Although the reactivity of most organic pollutants (i.e., diquat, atrazine and deethylatrazine) with $\bullet O_2^-$ are significantly lower than that with •OH on account of the lower oxidation potential of $\bullet O_2^-$ (($E^0(\bullet O_2^-/H_2O_2) = 0.93$ V vs ($E^0(\bullet OH/H_2O) = 2.72$ V)/($E^0(\bullet OH/OH^-) = 1.89$ V)) [114,115]. It should be noted that $\bullet O_2^-$ could react actively with some electrophilic compounds (i.e., quinone derivatives, CCl_4, chloroform ($CHCl_3$), and hexachlorobenzene (C_6Cl_6)) due to its strong nucleophilicity (Eqs. 16–17) [37,40,113]. For example, Sawyer proposed a possible reaction mechanism between C_6Cl_6 and $\bullet O_2^-$, where $\bullet O_2^-$ would react with C_6Cl_6 through nucleophilic addition and then lead to the loss of chloride (Cl^-) (Fig. 9(A)) [41]. Meanwhile, some studies also proposed that $\bullet O_2^-$ could lead to the degradation of perfluorooctanoic acid (PFOA) by firstly nucleophilic attacking the C-F bond, followed by $\bullet O_2^-$-mediated decarboxylation [116,117]. Nevertheless, this may be achieved with the assistance of multiple reactive species since Javed et al., found that $\bullet O_2^-$ alone played no significant role in PFOA degradation [118]. Meanwhile, it is worth noting that the reactivity of $\bullet O_2^-$ in compound less polar than water (i.e., H_2O_2, ethylene glycol, and acetone) was higher than that in deionized water, which may be related to the altering of solvation shell [119].

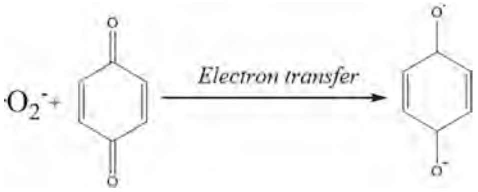

$$\cdot O_2^- + RX \rightarrow \left[\cdot O_2^- \cdots R \cdots X \rightleftharpoons O_2 \cdots R \cdots X^-\right] \xrightarrow{Nucleophilic\ \ substitution} RO_2^{\cdot} + X^- \tag{17}$$

Recently, most of studies also proposed that $\bullet O_2^-$ could be reckoned as the precursor for $^1O_2$, and the pathway essentially involved the recombination of $\bullet O_2^-$/ $HO_2\bullet$ (Eqs. 18–19), the interaction of $\bullet O_2^-$ with •OH (Eq. (20)), or electron transfer from $\bullet O_2^-$ to surface metal sites [27,120–122]. As a non-radical species, $^1O_2$ is possible to selectively react with most unsaturated organic pollutants as well as sulfide and amine groups via electrophilic addition or electron transfer (Fig. 7), while shows negligible reactivity toward saturated alcohol owing to its electrophilic nature [123,124]. For example, the addition of $^1O_2$ to benzene ring of isoproturon has been reported by researchers [125]. Additionally, Barrios et al., carefully studied the reaction mechanisms of $^1O_2$ with various organic compounds through DFT calculations, where the mechanisms mainly involved single electron transfer and addition (Eqs. 21–22). As can be seen from Fig. 9(B), phenolates underwent both single electron transfer (dissociated OH group) and $^1O_2$ addition reactions, while phenols primarily underwent $^1O_2$ addition reaction. Meanwhile, $^1O_2$ tended to addition to the five-membered ring of furan derivatives, and reacted with imidazole and the derivatives through 1,4-addition. As for aliphatic amines, the single electron transfer was considered to be the dominant mechanism [39]. This study provided an available guidance for better understanding the reaction between $^1O_2$ and organic pollutants. Moreover, owing to this kind of "substrate-

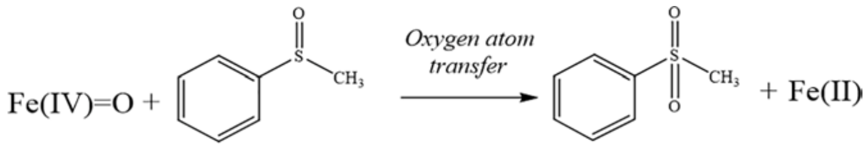

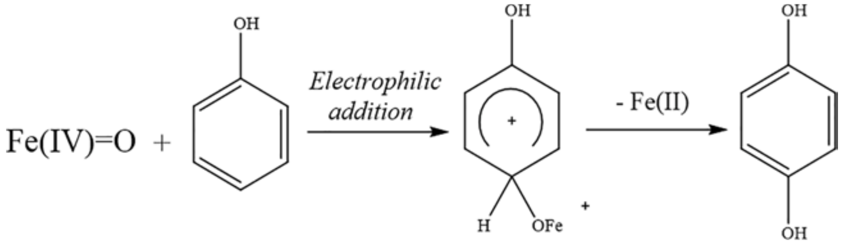

dependent" oxidation effect, $^1O_2$-induced organic pollutants degradation process can suffer less interference from background substances in water (i.e., organic matters and coexisting ions). However, due to its mild oxidation potential ($E^0(^1O_2/\bullet O_2^-) = 0.81$ V), the depletion of total organic carbon (TOC) by $^1O_2$ seems to be impossible [61,111].

$$\cdot O_2^- + HO_2\cdot + H^+ \rightarrow {}^1O_2 + H_2O_2 \tag{18}$$

$$2\cdot O_2^- + 2H_2O \rightarrow {}^1O_2 + H_2O_2 + 2OH^- \tag{19}$$

$$\cdot OH + \cdot O_2^- \rightarrow OH^- + 1O_2 \tag{20}$$

$$1O_2 + R \rightarrow [1O_2R^{\cdot -}\cdots R^{\cdot}] \xleftarrow{Single\ electron\ transfer} \left[1O_2^{\cdot -}\cdots R^{\cdot +}\right]^{\neq} \rightarrow \cdot O_2^- + R^{\cdot +} \tag{21}$$

$$1O_2 + R \rightarrow \left[1O_2{}^{\cdot -}\cdots R^{\cdot +}\right] \xrightarrow{Addition} [O_2\cdots R]^{\neq} \rightarrow O - O - R \tag{22}$$

Where $\left[1O_2{}^{\cdot -}\cdots R^{+}\right]$ represented the precursor complex, $\left[1O_2^{\cdot -}\cdots R^{\cdot +}\right]^{\neq}$ and $[O_2\cdots R]^{\neq}$ represented the transition states.

3.2.2. Fe(IV) = O/Fe(V) = O

As another non-radical species, Fe(IV) = O/Fe(V) = O are also regarded as potential oxidants to selectively destruct organic pollutants during Fe-based Fenton-like reactions. Taking Fe(IV) = O as example, several studies have reported that the highly electrophilic Fe(IV) = O tended to react with organic pollutants comprising electron-rich groups (i.e., hydroxyl, amino, and methyl groups) through various reaction pathways (Fig. 7) including hydrogen atom transfer, hydride transfer, oxygen atom transfer, and electrophilic addition (Eqs. 23–26) [29,38,105]. For instance, Pan et al. proposed that during the process of tetracycline degradation, Fe(IV) = O firstly attacked the electron-donating groups on tetracycline through oxygen/hydrogen atom transfer process, and then leading to the further destruction [126]. It was also reported that the degradation of phenol, nitrobenzene, and nitrophenols by Fe(IV) = O was initially achieved by electrophilic addition of Fe(IV) = O on the aromatic rings [127]. Besides, Pestovsky et al., studied the effects of substituent groups on the reaction rate between benzyl alcohols and Fe(IV) = O. They revealed that benzyl alcohols substituted with electron-donating groups such as p-CH_3O-C_6H_4-CH_2OH ($k = 1.59 \times 10^4$ M^{-1} s^{-1}) and p-CH_3-C_6H_4-CH_2OH ($k = 1.50 \times 10^4$ M^{-1} s^{-1}) exhibited higher reaction rate than that substituted with electron-withdrawing groups such as p-Br-C_6H_4-CH_2OH ($k = 1.41 \times 10^4$ M^{-1} s^{-1}) and p-CF_3-C_6H_4-CH_2OH ($k = 1.00 \times 10^4$ M^{-1} s^{-1}), which indicated that the electron-withdrawing groups (-CF_3 and -Br) exhibited mild negative impacts, and the electron-donating groups (–OCH_3 and –CH_3) moderately accelerated the reactions [128].

$$\begin{aligned} Fe(IV) = O + R_nCH - OH &\xrightarrow{\substack{Hydrogen\ atom \\ transfer}} Fe(III)OH + R_nC^{\cdot} - OH \\ &\times \xrightarrow{+\ O_2} R_nC \\ &= O + HO_2 \end{aligned} \tag{23}$$

$$\begin{aligned} \mathrm{Fe(IV) = O + R_nCH\text{-}OH} &\xrightarrow{\text{Hydride transfer}} \mathrm{Fe(II)OH + R_nC} \\ &= \mathrm{O + H_2O} \end{aligned} \tag{24}$$

Meanwhile, the "substrate-dependent" oxidation effect of Fe(IV) = O offers available opportunities to differentiate Fe(IV) = O and •OH during Fenton-like reactions. To be specific, it was reported that oxy-compounds of arsenic, selenium, nitrogen, and sulfur were more likely to undergo an oxygen-atom transfer step when oxidizing by Fe(IV) = O, markedly differing from their •OH-induced oxidation [129]. For instance, PMSO and DMSO were usually oxidized to corresponding sulfone ($PMSO_2$ and $DMSO_2$) by Fe(IV) = O. While •OH would oxidize PMSO to hydroxylated products, and DMSO to ethane and methyl sulfinic acid [105,130]. In this regard, it is capable of distinguishing Fe(IV) = O and •OH during reaction by comparing the formed products. Nevertheless, because the rate constant between •OH and PMSO/DMSO is relatively higher than that between Fe(IV) = O and PMSO/DMSO, it is recommended to use excessive PMSO/DMSO to eliminate the interference of •OH during such process [59,60]. Recently, Dong et al. also proposed a novel diagnostic method for clarifying the role of •OH and Fe(IV) by comparing the molar ratio of formed intermediates desisopropyl-atrazine (DIA) and desethyl-atrazine (DEA) during atrazine oxidation (Fig. 9(C)). Since Fe(IV) = O tended to attract *N*-ethyl functional group of atrazine, the ratio of DEA to DIA was about 7.5 in the system dominated by Fe(IV) = O and decreased to 2.0 when •OH was the primary oxidant [131]. Moreover, it is precisely because of this selective degradation mechanism, Fe(IV) = O species could be less interfered by background substances in wastewater treatment just like $^1O_2$. While Fe(IV) = O species also shows unfavorable mineralization ability although its oxidation potential is relatively higher ($E^0(Fe^{IV} = O^{2+}, H^+/Fe^{III}OH^{2+}) \geq 1.95$ V, $E^0(Fe^{IV} = O^{2+}/Fe^{III}O^+) > 1.3$ V) [77,132].

Overall, in Fe-based Fenton-like systems, the selective degradation of organic pollutants can be achieved by regulating the existing form of •OH, or generation of Fe(IV) = O/Fe(V) = O, $\bullet O_2^-$, and $^1O_2$ according to the chemical properties of organic pollutants. To achieve this, it is significant to identify the reactive species during reactions, and many approaches have been proposed [61,104,133]. For example, electron

Table 1
The commonly used methods and probes for reaction species detection.

Reactive species	Detection methods	Probe	Reference
•OH	EPR	DMPO	[120]
	Spectrophotometry	DMSO	[133]
	Fluorescence	Coumarin	[139]
	Chemiluminescence	Phthalhydrazide	[134]
	HPLC	Salicylic acid	[140]
		Benzoic acid	[141]
•O_2^-	EPR	DMPO	[79]
	Spectrophotometry	Nitrotetrazolium blue chloride (NBT)	[115]
	Fluorescence	4-Chloro-7-nitro-1,2,3-benzoxadiazole (NBD-Cl)	[135]
		Diketopyrrolopyrrole derivates	[142]
	Chemiluminescence	5-amino-2,3-dihydroxy-1,4-Phthalazinedione (luminol)	[134]
		Methoxy cypridina luciferin analog (MCLA)	[143]
$^1O_2$	EPR	TEMP	[121]
	Spectrophotometry	9,10-diphenylanthracene (DPA)	[144]
		1,3-diphenylisobenzofuran (DPBF)	[120]
	Fluorescence	9-[2-(3-carboxy-9,10-dimethyl) anthryl]-6-hydroxy-3H-xanthen-3-one (DMAX)	[145]
	Chemiluminescence	Tetrathiafulvalenem (TTF) -substituted anthracene probe	[146]
	HPLC	FFA	[147]
		Metronidazole (MDE)	[138]
Fe(IV) = O/ Fe(V) = O	HPLC	PMSO	[129]
	GC–MS	DMSO	[130]

paramagnetic resonance (EPR) technology has been widely employed to detect •OH and •O_2^- by using a spin trap 5,5-dimethyl-1-pyrroline-*N*-oxide (DMPO) [26,79], and $^1O_2$ by using a spin trap 4-oxo-2,2,6,6-tetramethylpiperidine (TEMP) [120]. The appearance of DMPO-•OH, DMPO-•O_2^-, and TEMP-$^1O_2$ signal verifies the existence of •OH, •O_2^-, and $^1O_2$, respectively. Apart from that, some other strategies including spectrophotometry, fluorescence, high performance liquid chromatography (HPLC), gas chromatography-mass spectrum (GC–MS) and chemiluminescence methods are also commonly used for reactive species detection [106,133–135]. As for spectrophotometry, fluorescence, HPLC and GC–MS methods, a suitable probe compound is generally utilized to react with a certain reactive species, and the presence of such reactive species is reflected by the production of corresponding adduct, which can be detected though a separate detection step. For chemiluminescence method, light will be immediately emitted when a chemiluminescence probe is mixed with a certain reactive species, therefore verifying the existence of the reactive species. The commonly used probe compounds in these strategies have been summarized in Table 1. In addition to the detection of reactive species, the contribution of one reactive species during catalytic reaction can also be distinguished by suppressing the role of this reactive species with corresponding quenching agents. However, some drawbacks of such method still exist, such as the interference of other reactive species, and changes of reaction mechanisms caused by high concentration of quenching agents [136–138]. The detailed information is summarized in Table 2. In this case, probe approach is proposed as an alternative to investigate the role of reactive species [61,115]. During such process, the concentration of reactive species can be reflected by measuring the concentration of corresponding products between reactive species and probes. On the basis of the measured reactive species concentration and chemical kinetic models, the relative contribution of reactive species to pollutants degradation can be possibly estimated.

Table 2
The summary of commonly used quenching methods for •OH, •O_2^-, $^1O_2$ and Fe (IV) = O/Fe(V) = O.

Reactive species	Detection method	Drawbacks	Reference
•OH	Alcohols (i.e., *tert*-butanol, isopropanol, *n*-propanol, methanol, and ethanol)	(1) The reaction between alcohols and •OH will resulting the re-formation of H_2O_2 in the presence of molecular oxygen, the order is decreased as methanol > ethanol > isopropanol > *n*-propanol > *tert*-butanol; (2) Alcohols may scavenge •OH bound to surface or in the bulk solution depending on their affinity to catalyst surface, while the interaction of each alcohol and a certain catalyst surface are different, making it difficult to generalize.	[104,136]
	KI	KI is usually employed as scavengers of surface-bound •OH, while the reaction between KI and Fe or KI and H_2O_2 may interfere with the quenching result.	[61]
•O_2^-	Benzoquinone (BQ)	(1) BQ has low solubility in water, which cannot completely quench the •O_2^-; (2) •OH is quite active for attacking BQ and therefore have an impact on the quenching results.	[111,138]
	2,2,6,6-tetramethylpiperidine (TEMPOL)	TEMPOL can also react with •OH and exhibits catalase activity, which could lead to an inaccurate quenching effect.	[148]
	Chloroform	(1) $CHCl_3$ has low solubility in water, which could affect its quenching effect on •O_2^-; (2) The volatilization of $CHCl_3$ will significantly complicate the calculation of •O_2^- exposure.	[61,115]
	Superoxide dismutase (SOD)	The inhibition mechanism of SOD towards •O_2^- will lead to radical •OH generation.	[149]
$^1O_2$	Furfuryl alcohol (FFA)	FFA is also highly reactive toward •OH. Therefore, failure to add a •OH quencher when quenching $^1O_2$ would result in an overestimation of $^1O_2$ concentration.	[138]
	Sodium azide (NaN_3)	(1) NaN_3 is a reducing agent. In addition to quenching $^1O_2$, it can also react with some oxidants such as H_2O_2.	[61,150]

(*continued on next page*)

Table 2 (*continued*)

Reactive species	Detection method	Drawbacks	Reference
		For this reason, the concentration of NaN_3 should not be very high to reduce the reaction between NaN_3 and H_2O_2; (2) NaN_3 also can react with other active species such as $\bullet OH$ and $\bullet O_2^-$.	
	L-histidine (L-His)	(1) L-His can react with $\bullet OH$, which might mislead the quenching result of $^1O_2$; (2) The addition of L-His may slight decrease the solution pH and cause effect on catalytic process.	[137]
Fe(IV) = O/Fe (V) = O	PSMO/DMSO	(1) PMSO and DMSO can react with $\bullet OH$ and therefore interfere with their reaction with Fe (IV) = O/Fe(V) = O and generation of $PMSO_2$/$DMSO_2$; (2) The generated $PMSO_2$/$DMSO_2$ can also react with $\bullet OH$ in a high reaction rate, which may affect the accurate detection of $PMSO_2$ and $DMSO_2$.	[58,59]

4. Conclusions and perspectives

Heterogeneous Fenton-like processes have been extensively studied over the past few years. During such processes, organic pollutants will react with the generated reactive species and then being decomposed. Therefore, a firm understanding of the fundamentals of the reactive species generation and utilization is significant for improving Fenton-like performance.

In this review, the mechanisms of H_2O_2 decomposition at surface Fe sites (Fe^0, Fe(II), and Fe(III)), oxygen vacancies, as well as electron-polarized micro-areas have been briefly discussed with specific attention to reactive species (i.e., Fe(IV) = O/Fe(V) = O, $\bullet OH$, $\bullet O_2^-$ and $^1O_2$) production. Nevertheless, it remains challenging to elucidate the detailed processes of reactive species generation. For example, a unified and clear reaction mechanism for inducing peroxide O—O bond heterolysis in Fe(II)–H_2O_2 complex to produce Fe(IV) = O is still lacking. Therefore, a more precise elucidation of the interaction between H_2O_2 and the active site is still needed, which can be achieved by combining multiple methods, such as in-situ EPR, XAFS, and DFT to further determine key information about the activation mechanism, including variation of electron density, coordination configuration, bond formation, bond length, H_2O_2 dissociated energy barrier, etc.

Besides, although the selective degradation processes can be achieved through regulating the generation of a certain reactive species, it is still challenging to balance the selective degradation and mineralization rates, because the intermediate products generated after the target pollutants being selectively attacked may not be further degraded. The simultaneous existence of reactive species with lower oxidation potential but high selectivity to target organic pollutants, and $\bullet OH$ with high oxidation potential but low selectivity may be beneficial for achieving a high mineralization rate in complex aqueous substrates, which is a sought research direction for future study.

Meanwhile, as discussed before, the contribution of a certain reactive species is usually obtained through quenching experiments in current study. However, the complications and uncertainties arising from the consumption of scavengers by multiple reactive species, and unexpected reactions (i.e., re-formation of H_2O_2 and $\bullet OH$) triggered by high concentration of quenching agents may mislead the quenching results. Other means, such as combining probe-based kinetic models, are suggested when applying the quenching experiments to interpret the role of reactive species to assure the reliability of results.

Declaration of Competing Interest

The authors declare that they have no known competing financial interests or personal relationships that could have appeared to influence the work reported in this paper.

Data availability

Data will be made available on request.

Acknowledgments

This study was financially supported by the Program for the National Natural Science Foundation of China (51521006, 51779090, 51879101, 51579098, 51709101, 51809090, 51909084), the National Program for Support of Top-Notch Young Professionals of China (2014), the Program for Changjiang Scholars and Innovative Research Team in University (IRT-13R17), and Hunan Natural Science Foundation (2020JJ3009), Hunan Researcher Award Program (2020RC3025), Hunan Provincial Science and Technology Plan Project (2018SK20410, 2017SK2243, 2016RS3026), and the Fundamental Research Funds for the Central Universities (531118010247, 531118040083).

Appendix A. Supplementary data

Supplementary data to this article can be found online at https://doi.org/10.1016/j.cej.2022.140126.

References

[1] N. Barhoumi, H. Olvera-Vargas, N. Oturan, D. Huguenot, A. Gadri, S. Ammar, E. Brillas, M.A. Oturan, Kinetics of oxidative degradation/mineralization pathways of the antibiotic tetracycline by the novel heterogeneous electro-Fenton process with solid catalyst chalcopyrite, Appl. Catal. B: Environ. 209 (2017) 637–647, https://doi.org/10.1016/j.apcatb.2017.03.034.

[2] J. Tang, J. Wang, Iron-copper bimetallic metal-organic frameworks for efficient Fenton-like degradation of sulfamethoxazole under mild conditions, Chemosphere 241 (2020), 125002, https://doi.org/10.1016/j.chemosphere.2019.125002.

[3] Y. Liu, Y. Chen, J. Deng, J. Wang, N-doped aluminum-graphite (Al-Gr-N) composite for enhancing in-situ production and activation of hydrogen peroxide to treat landfill leachate, Appl. Catal. B: Environ. 297 (2021), 120407, https://doi.org/10.1016/j.apcatb.2021.120407.

[4] J. Wang, J. Tang, Fe-based Fenton-like catalysts for water treatment: Preparation, characterization and modification, Chemosphere 276 (2021), 130177, https://doi.org/10.1016/j.chemosphere.2021.130177.

[5] X. Wang, X. Zhang, Y. Zhang, Y. Wang, S.-P. Sun, W.D. Wu, Z. Wu, Nanostructured semiconductor supported iron catalysts for heterogeneous photo-Fenton oxidation: a review, J. Mater. Chem. A 8 (31) (2020) 15513–15546, https://doi.org/10.1039/D0TA04541A.

[6] J. Wang, J. Tang, Fe-based Fenton-like catalysts for water treatment: Catalytic mechanisms and applications, J. Mol. Liq. 332 (2021), 115755, https://doi.org/10.1016/j.molliq.2021.115755.

[7] J. Barrault, C. Bouchoule, J.-M. Tatibouët, M. Abdellaoui, A. Majesté, I. Louloudi, N. Papayannakos, N. Gangas, Catalytic wet peroxide oxidation over mixed (Al-Fe) pillared clays, Stud. Surf. Sci. Catal. 130 (2000) 749–754, https://doi.org/10.1016/S0167-2991(00)81048-4.

[8] C. Pulgarin, P. Peringer, P. Albers, J. Kiwi, Effect of Fe-ZSM-5 zeolite on the photochemical and biochemical degradation of 4-nitrophenol, J. Mol. Catal. A: Chem. 95 (1) (1995) 61–74, https://doi.org/10.1016/1381-1169(94)00156-1.

[9] M. Berger, M. De Hazen, A. Nejjari, J. Fournier, J. Gulgnard, H. Pezerat, J. Cadet, Radical oxidation reaction of the purine moiety of 2′-deoxyribonucleosides and DNA by iron-containing minerals, Carcinogenesis 14 (1) (1993) 41–46, https://doi.org/10.1093/carcin/14.1.41.

[10] R.J. Watts, M.D. Udell, P.A. Rauch, S.W. Leung, Treatment of pentachlorophenol-contaminated soils using Fenton's reagent, Hazard. Waste Hazard. Mater. 7 (4) (1990) 335–345, https://doi.org/10.1089/hwm.1990.7.335.

[11] S. Bhattacharjee, J.-S. Choi, S.-T. Yang, S.B. Choi, J. Kim, W.-S. Ahn, Solvothermal synthesis of Fe-MOF-74 and its catalytic properties in phenol hydroxylation, J. Nanosci. Nanotechnol. 10 (1) (2010) 135–141, https://doi.org/10.1166/jnn.2010.1493.

[12] J.M. Gutteridge, L. Maidt, L. Poyer, Superoxide dismutase and Fenton chemistry. Reaction of ferric-EDTA complex and ferric-bipyridyl complex with hydrogen peroxide without the apparent formation of iron (II), Biochem. J. 269 (1) (1990) 169–174, https://doi.org/10.1042/bj2690169.

[13] L.S. Hundal, J. Singh, E.L. Bier, P.J. Shea, S.D. Comfort, W.L. Powers, Removal of TNT and RDX from water and soil using iron metal, Environ. Pollut. 97 (1) (1997) 55–64, https://doi.org/10.1016/S0269-7491(97)00081-X.

[14] K. Fajerwerg, H. Debellefontaine, Wet oxidation of phenol by hydrogen peroxide using heterogeneous catalysis Fe-ZSM-5: a promising catalyst, Appl. Catal. B: Environ. 10 (4) (1996) 229–235, https://doi.org/10.1016/S0926-3373(96)00041-0.

[15] N. Al-Hayek, M. Dore, Oxidation of phenols in water by hydrogen peroxide on alumina supported iron, Water Res. 24 (8) (1990) 973–982, https://doi.org/10.1016/0043-1354(90)90119-Q.

[16] M.Y. El-Sheikh, F.M. Ashmawy, I.A. Salem, A.B. Zaki, U. Nickel, Catalytic decomposition of hydrogen peroxide in the presence of N, N′-bis (salicylidene)-o-phenylenediamineiron (III) sorbed on to Dowex-50W resin, Transit. Metal Chem. 16 (3) (1991) 319–323, https://doi.org/10.1007/BF01024073.

[17] W. Luo, L. Zhu, N. Wang, H. Tang, M. Cao, Y. She, Efficient removal of organic pollutants with magnetic nanoscaled $BiFeO_3$ as a reusable heterogeneous Fenton-like catalyst, Environ. Sci. Technol. 44 (5) (2010) 1786–1791, https://doi.org/10.1021/es903390g.

[18] X.-J. Yang, X.-M. Xu, J. Xu, Y.-F. Han, Iron oxychloride (FeOCl): An efficient Fenton-like catalyst for producing hydroxyl radicals in degradation of organic contaminants, J. Am. Chem. Soc. 135 (43) (2013) 16058–16061, https://doi.org/10.1021/ja409130c.

[19] S. An, G. Zhang, T. Wang, W. Zhang, K. Li, C. Song, J.T. Miller, S. Miao, J. Wang, X. Guo, High-density ultra-small clusters and single-atom Fe sites embedded in graphitic carbon nitride ($g-C_3N_4$) for highly efficient catalytic advanced oxidation processes, ACS Nano 12 (9) (2018) 9441–9450, https://doi.org/10.1021/acsnano.8b04693.

[20] J. Tang, J. Wang, Metal organic framework with coordinatively unsaturated sites as efficient Fenton-like catalyst for enhanced degradation of sulfamethazine, Environ. Sci. Technol. 52 (9) (2018) 5367–5377, https://doi.org/10.1021/acs.est.8b00092.

[21] Z. Han, X. Han, X. Zhao, J. Yu, H. Xu, Iron phthalocyanine supported on amidoximated PAN fiber as effective catalyst for controllable hydrogen peroxide activation in oxidizing organic dyes, J. Hazard. Mater. 320 (2016) 27–35, https://doi.org/10.1016/j.jhazmat.2016.08.004.

[22] N. Barhoumi, N. Oturan, H. Olvera-Vargas, E. Brillas, A. Gadri, S. Ammar, M. A. Oturan, Pyrite as a sustainable catalyst in electro-Fenton process for improving oxidation of sulfamethazine. Kinetics, mechanism and toxicity assessment, Water Res. 94 (2016) 52–61, https://doi.org/10.1016/j.watres.2016.02.042.

[23] Y. Zhuang, Q. Liu, Y. Kong, C. Shen, H. Hao, D.D. Dionysiou, B. Shi, Enhanced antibiotic removal through a dual-reaction-center Fenton-like process in 3D graphene based hydrogels, Environ. Sci. Nano 6 (2019) 388–398, https://doi.org/10.1039/C8EN01339J.

[24] W. Xu, W. Xue, H. Huang, J. Wang, C. Zhong, D. Mei, Morphology controlled synthesis of $\alpha-Fe_2O_{3-x}$ with benzimidazole-modified Fe-MOFs for enhanced photo-Fenton-like catalysis, Appl. Catal. B: Environ. 291 (2021), 120129, https://doi.org/10.1016/j.apcatb.2021.120129.

[25] M.K. Panjwani, Q. Wang, Y. Ma, Y. Lin, F. Xiao, S. Yang, High degradation efficiency of sulfamethazine with the dual-reaction-center Fe-Mn-SiO_2 Fenton-like nanocatalyst in a wide pH range, Environ. Sci. Nano 8 (2021) 2204–2213, https://doi.org/10.1039/D1EN00253H.

[26] R.-R. Ding, W.-Q. Li, C.-S. He, Y.-R. Wang, X.-C. Liu, G.-N. Zhou, Y. Mu, Oxygen vacancy on hollow sphere $CuFe_2O_4$ as an efficient Fenton-like catalysis for organic pollutant degradation over a wide pH range, Appl. Catal. B: Environ. 291 (2021), 120069, https://doi.org/10.1016/j.apcatb.2021.120069.

[27] Y. Yin, Y. Ren, J. Lu, W. Zhang, C. Shan, M. Hua, L. Lv, B. Pan, The nature and catalytic reactivity of UiO-66 supported Fe_3O_4 nanoparticles provide new insights into Fe-Zr dual active centers in Fenton-like reactions, Appl. Catal. B: Environ. 286 (2021), 119943, https://doi.org/10.1016/j.apcatb.2021.119943.

[28] M. Sun, C. Chu, F. Geng, X. Lu, J. Qu, J. Crittenden, M. Elimelech, J.-H. Kim, Reinventing Fenton chemistry: iron oxychloride nanosheet for pH-insensitive H_2O_2 activation, Environ. Sci. Tech. Let. 5 (3) (2018) 186–191, https://doi.org/10.1021/acs.estlett.8b00065.

[29] J. He, X. Yang, B. Men, D. Wang, Interfacial mechanisms of heterogeneous Fenton reactions catalyzed by iron-based materials: a review, J. Environ. Sci. 39 (2016) 97–109, https://doi.org/10.1016/j.jes.2015.12.003.

[30] C.R. Keenan, D.L. Sedlak, Factors affecting the yield of oxidants from the reaction of nanoparticulate zero-valent iron and oxygen, Environ. Sci. Technol. 42 (4) (2008) 1262–1267, https://doi.org/10.1021/es7025664.

[31] I.A. Katsoyiannis, T. Ruettimann, S.J. Hug, pH dependence of Fenton reagent generation and As(III) oxidation and removal by corrosion of zero valent iron in aerated water, Environ. Sci. Technol. 42 (19) (2008) 7424–7430, https://doi.org/10.1021/es800649p.

[32] S.-Y. Pang, J. Jiang, J. Ma, Response to comment on "Oxidation of sulfoxides and arsenic(III) in corrosion of nanoscale zero valent iron by oxygen: Evidence against ferryl ions (Fe(IV)) as active intermediates in Fenton reaction", Environ. Sci. Technol. 45 (7) (2011) 3179–3180, https://doi.org/10.1021/es2004304.

[33] S.-Y. Pang, J. Jiang, J. Ma, Oxidation of sulfoxides and arsenic(III) in corrosion of nanoscale zero valent iron by oxygen: evidence against ferryl ions (Fe(IV)) as active intermediates in Fenton reaction, Environ. Sci. Technol. 45 (1) (2011) 307–312, https://doi.org/10.1021/es102401d.

[34] Y. Chen, C.J. Miller, T.D. Waite, pH dependence of hydroxyl radical, ferryl, and/or ferric peroxo species generation in the heterogeneous Fenton process, Environ. Sci. Technol. 56 (2) (2022) 1278–1288, https://doi.org/10.1021/acs.est.1c05722.

[35] W. Shuai, C. Gu, G. Fang, D. Zhou, J. Gao, Effects of iron (hydr)oxides on the degradation of diethyl phthalate ester in heterogeneous (photo)-Fenton reactions, J. Environ. Sci. 80 (2019) 5–13, https://doi.org/10.1016/j.jes.2018.06.015.

[36] T. Jiang, A.S. Poyraz, A. Iyer, Y. Zhang, Z. Luo, W. Zhong, R. Miao, A.M. El-Sawy, C.J. Guild, Y. Sun, D.A. Kriz, S.L. Suib, Synthesis of mesoporous iron oxides by an inverse micelle method and their application in the degradation of Orange II under visible light at neutral pH, J. Phys. Chem. C 119 (19) (2015) 10454–10468, https://doi.org/10.1021/acs.jpcc.5b02057.

[37] B.A. Smith, A.L. Teel, R.J. Watts, Identification of the reactive oxygen species responsible for carbon tetrachloride degradation in modified Fenton's systems, Environ. Sci. Technol. 38 (20) (2004) 5465–5469, https://doi.org/10.1021/es0352754.

[38] H. Chen, T. Lin, W. Chen, H. Xu, H. Tao, Significant role of high-valent iron-oxo species in the degradation and detoxification of indomethacine, Chemosphere 251 (2020), 126451, https://doi.org/10.1016/j.chemosphere.2020.126451.

[39] B. Barrios, B. Mohrhardt, P.V. Doskey, D. Minakata, Mechanistic insight into the reactivities of aqueous-phase singlet oxygen with organic compounds, Environ. Sci. Technol. 55 (12) (2021) 8054–8067, https://doi.org/10.1021/acs.est.1c01712.

[40] Z. Luo, M.-Y. Tseng, D. Minakata, L. Bai, W.-P. Hu, W. Song, Z. Wei, R. Spinney, D.D. Dionysiou, R. Xiao, Mechanistic insight into superoxide radical-mediated degradation of carbon tetrachloride in aqueous solution: an in situ spectroscopic and computational study, Chem. Eng. J. 410 (2021), 128181, https://doi.org/10.1016/j.cej.2020.128181.

[41] H. Sugimoto, S. Matsumoto, D.T. Sawyer, Oxygenation of polychloro aromatic hydrocarbons by superoxide ion in aprotic media, J. Am. Chem. Soc. 109 (26) (1987) 8081–8082, https://doi.org/10.1021/ja00260a021.

[42] Z. Yang, J. Qian, C. Shan, H. Li, Y. Yin, B. Pan, Toward selective oxidation of contaminants in aqueous systems, Environ. Sci. Technol. 55 (21) (2021) 14494–14514, https://doi.org/10.1021/acs.est.1c05862.

[43] L. Chen, S. Wang, Z. Yang, J. Qian, B. Pan, Selective interfacial oxidation of organic pollutants in Fenton-like system mediated by Fe(III)-adsorbed carbon nanotubes, Appl. Catal. B: Environ. 292 (2021), 120193, https://doi.org/10.1016/j.apcatb.2021.120193.

[44] N. Farhadian, S. Liu, A. Asadi, M. Shahlaei, S. Moradi, Enhanced heterogeneous Fenton oxidation of organic pollutant via Fe-containing mesoporous silica composites: a review, J. Mol. Liq. 321 (2021), 114896, https://doi.org/10.1016/j.molliq.2020.114896.

[45] M. Munoz, Z.M. de Pedro, J.A. Casas, J.J. Rodriguez, Preparation of magnetite-based catalysts and their application in heterogeneous Fenton oxidation-A review, Appl. Catal. B: Environ. 176–177 (2015) 249–265, https://doi.org/10.1016/j.apcatb.2015.04.003.

[46] S. Rahim Pouran, A.A. Abdul Raman, W.M.A. Wan Daud, Review on the application of modified iron oxides as heterogeneous catalysts in Fenton reactions, J. Clean. Prod. 64 (2014) 24–35, https://doi.org/10.1016/j.jclepro.2013.09.013.

[47] Y. Zhu, R. Zhu, Y. Xi, J. Zhu, G. Zhu, H. He, Strategies for enhancing the heterogeneous Fenton catalytic reactivity: a review, Appl. Catal. B: Environ. 255 (2019), 117739, https://doi.org/10.1016/j.apcatb.2019.05.041.

[48] N. Thomas, D.D. Dionysiou, S.C. Pillai, Heterogeneous Fenton catalysts: a review of recent advances, J. Hazard. Mater. 404 (2021), 124082, https://doi.org/10.1016/j.jhazmat.2020.124082.

[49] I. Magario, F.S.G. Einschlag, E.H. Rueda, J. Zygadlo, M.L. Ferreira, Mechanisms of radical generation in the removal of phenol derivatives and pigments using different Fe-based catalytic systems, J. Mol. Catal. A-Chem. 352 (2012) 1–20, https://doi.org/10.1016/j.molcata.2011.10.006.

[50] Y. Liu, Y. Zhao, J. Wang, Fenton/Fenton-like processes with in-situ production of hydrogen peroxide/hydroxyl radical for degradation of emerging contaminants: advances and prospects, J. Hazard. Mater. 404 (2021), 124191, https://doi.org/10.1016/j.jhazmat.2020.124191.

[51] J. Du, W. Guo, X. Li, Q. Li, B. Wang, Y. Huang, N. Ren, Degradation of sulfamethoxazole by a heterogeneous Fenton-like system with microscale zero-valent iron: kinetics, effect factors, and pathways, J. Taiwan Inst. Chem. E. 81 (2017) 232–238, https://doi.org/10.1016/j.jtice.2017.10.017.

[52] Y. Sun, J. Li, T. Huang, X. Guan, The influences of iron characteristics, operating conditions and solution chemistry on contaminants removal by zero-valent iron: a review, Water Res. 100 (2016) 277–295, https://doi.org/10.1016/j.watres.2016.05.031.

[53] Y. Yang, L. Xu, W. Li, W. Fan, S. Song, J. Yang, Adsorption and degradation of sulfadiazine over nanoscale zero-valent iron encapsulated in three-dimensional graphene network through oxygen-driven heterogeneous Fenton-like reactions, Appl. Catal. B: Environ. 259 (2019), 118057, https://doi.org/10.1016/j.apcatb.2019.118057.

[54] Z. Wan, J. Wang, Ce-Doped zero-valent iron nanoparticles as a Fenton-like catalyst for degradation of sulfamethazine, RSC Adv. 6 (105) (2016) 103523–103531, https://doi.org/10.1039/C6RA23709F.

[55] C.R. Keenan, D.L. Sedlak, Ligand-enhanced reactive oxidant generation by nanoparticulate zero-valent iron and oxygen, Environ. Sci. Technol. 42 (18) (2008) 6936–6941, https://doi.org/10.1021/es801438f.

[56] A.W. Vermilyea, B.M. Voelker, Photo-Fenton reaction at near neutral pH, Environ. Sci. Technol. 43 (18) (2009) 6927–6933, https://doi.org/10.1021/es900721x.

[57] S.-Y. Pang, J. Jiang, J. Ma, S.-Y. Pang, F. Ouyang, New insight into the oxidation of arsenite by the reaction of zerovalent iron and oxygen. Comment on "pH dependence of Fenton reagent generation and As(III) oxidation and removal by corrosion of zero valent iron in aerated water", Environ. Sci. Technol. 43 (10) (2009) 3978–3979, https://doi.org/10.1021/es9004015.

[58] H. Bardouki, M.B. da Rosa, N. Mihalopoulos, W.U. Palm, C. Zetzsch, Kinetics and mechanism of the oxidation of dimethylsulfoxide (DMSO) and methanesulfinate (MSI−) by OH radicals in aqueous medium, Atmos. Environ. 36 (29) (2002) 4627–4634, https://doi.org/10.1016/S1352-2310(02)00460-0.

[59] Z. Wang, J. Jiang, S. Pang, Y. Zhou, C. Guan, Y. Gao, J. Li, Y. Yang, W. Qiu, C. Jiang, Is sulfate radical really generated from peroxydisulfate activated by iron (II) for environmental decontamination? Environ. Sci. Technol. 52 (19) (2018) 11276–11284, https://doi.org/10.1021/acs.est.8b02266.

[60] O. Pestovsky, A. Bakac, Aqueous ferryl(IV) ion: Kinetics of oxygen atom transfer to substrates and oxo exchange with solvent water, Inorg. Chem. 45 (2) (2006) 814–820, https://doi.org/10.1021/ic051868z.

[61] J. Wang, S. Wang, Reactive species in advanced oxidation processes: Formation, identification and reaction mechanism, Chem. Eng. J. 401 (2020), 126158, https://doi.org/10.1016/j.cej.2020.126158.

[63] P. Salgado, V. Melin, M. Albornoz, H. Mansilla, G. Vidal, D. Contreras, Effects of pH and substituted 1,2-dihydroxybenzenes on the reaction pathway of Fenton-like systems, Appl. Catal. B: Environ. 226 (2018) 93–102, https://doi.org/10.1016/j.apcatb.2017.12.035.

[64] H. Bataineh, O. Pestovsky, A. Bakac, pH-induced mechanistic changeover from hydroxyl radicals to iron(iv) in the Fenton reaction, Chem. Sci. 3 (5) (2012) 1594–1599, https://doi.org/10.1039/C2SC20099F.

[65] H. Lee, H.-J. Lee, D.L. Sedlak, C. Lee, pH-dependent reactivity of oxidants formed by iron and copper-catalyzed decomposition of hydrogen peroxide, Chemosphere 92 (6) (2013) 652–658, https://doi.org/10.1016/j.chemosphere.2013.01.073.

[66] Y. Yin, R. Lv, W. Zhang, J. Lu, Y. Ren, X. Li, L. Lv, M. Hua, B. Pan, Exploring mechanisms of different active species formation in heterogeneous Fenton systems by regulating iron chemical environment, Appl. Catal. B: Environ. 295 (2021), 120282, https://doi.org/10.1016/j.apcatb.2021.120282.

[67] A.-L.-T. Pham, C. Lee, F.M. Doyle, D.L. Sedlak, A silica-supported iron oxide catalyst capable of activating hydrogen peroxide at neutral pH values, Environ. Sci. Technol. 43 (23) (2009) 8930–8935, https://doi.org/10.1021/es902296k.

[68] D. Wu, Y. Chen, Z. Zhang, Y. Feng, Y. Liu, J. Fan, Y. Zhang, Enhanced oxidation of chloramphenicol by GLDA-driven pyrite induced heterogeneous Fenton-like reactions at alkaline condition, Chem. Eng. J. 294 (2016) 49–57, https://doi.org/10.1016/j.cej.2016.02.097.

[69] J. da Silveira Salla, K. da Boit Martinello, G.L. Dotto, E. García-Díaz, H. Javed, P.J.J. Alvarez, E.L. Foletto, Synthesis of citrate-modified $CuFeS_2$ catalyst with significant effect on the photo-Fenton degradation efficiency of bisphenol a under visible light and near-neutral pH, Colloid, Surface. A 595 (2020), 124679, https://doi.org/10.1016/j.colsurfa.2020.124679.

[70] K. Yamaguchi, Y. Watanabe, I. Morishima, Direct observation of the push effect on the oxygen-oxygen bond cleavage of acylperoxoiron (III) porphyrin complexes, J. Am. Chem. Soc. 115 (10) (1993) 4058–4065, https://doi.org/10.1021/ja00063a026.

[71] W. Nam, H.J. Han, S.-Y. Oh, Y.J. Lee, M.-H. Choi, S.-Y. Han, C. Kim, S.K. Woo, W. Shin, New insights into the mechanisms of O-O bond cleavage of hydrogen peroxide and tert-Alkyl hydroperoxides by iron(III) porphyrin complexes, J. Am. Chem. Soc. 122 (36) (2000) 8677–8684, https://doi.org/10.1021/ja994403e.

[72] Y. Xia, N. Li, W. Lu, W. Wang, Y. Yao, Z. Zhu, T. Xu, Y. Gu, W. Chen, High-valent iron-oxo species on pyridine-containing MWCNTs generated in a solar-induced H_2O_2 activation system for the removal of antimicrobials, Chemosphere 273 (2021), 129545, https://doi.org/10.1016/j.chemosphere.2021.129545.

[73] X. Chen, W. Lu, T. Xu, N. Li, Z. Zhu, G. Wang, W. Chen, Visible-light-assisted generation of high-valent iron-oxo species anchored axially on g-C_3N_4 for efficient degradation of organic pollutants, Chem. Eng. J. 328 (2017) 853–861, https://doi.org/10.1016/j.cej.2017.07.110.

[74] K. Cheaib, M.Q.E. Mubarak, K. Sénéchal-David, C. Herrero, R. Guillot, M. Clémancey, J.-M. Latour, S.P. de Visser, J.-P. Mahy, F. Banse, F. Avenier, Selective formation of an $Fe^{IV}O$ or an $Fe^{III}OOH$ intermediate from iron(II) and H_2O_2: controlled heterolytic versus homolytic oxygen-oxygen bond cleavage by the second coordination sphere, Angew. Chem. Int. Edit. 58 (3) (2019) 854–858, https://doi.org/10.1002/anie.201812724.

[75] R. Su, J. Sun, Y. Sun, K. Deng, D. Cha, D. Wang, Oxidative degradation of dye pollutants over a broad pH range using hydrogen peroxide catalyzed by FePz $(dtnCl_2)_4$, Chemosphere 77 (8) (2009) 1146–1151, https://doi.org/10.1016/j.chemosphere.2009.08.005.

[76] B. Ensing, F. Buda, E.J. Baerends, Fenton-like chemistry in water: oxidation catalysis by Fe(III) and H_2O_2, J. Phys. Chem. A 107 (30) (2003) 5722–5731, https://doi.org/10.1021/jp0267149.

[77] H.-H. Kim, H. Lee, D. Lee, Y.-J. Ko, H. Woo, J. Lee, C. Lee, A.-L.-T. Pham, Activation of hydrogen peroxide by a Titanium oxide-supported iron catalyst: evidence for surface Fe(IV) and is selectivity, Environ. Sci. Technol. 54 (23) (2020) 15424–15432, https://doi.org/10.1021/acs.est.0c04262.

[78] J. Kim, J. Wang, D.C. Ashley, V.K. Sharma, C.-H. Huang, Enhanced degradation of micropollutants in a peracetic acid-Fe(III) aystem with picolinic acid, Environ. Sci. Technol. 56 (7) (2022) 4437–4446, https://doi.org/10.1021/acs.est.1c08311.

[79] Y. Liu, Y. Chen, Y. Da, F. Xie, J. Wang, Advanced treatment of landfill leachate using integrated coagulation/ photo-Fenton process through in-situ generated nascent Al^{3+} and H_2O_2 by Cl, N co-doped aluminum-graphite composite, Appl. Catal. B: Environ. 304 (2022), 121003, https://doi.org/10.1016/j.apcatb.2021.121003.

[80] L. Li, S. Liu, M. Cheng, C. Lai, G. Zeng, L. Qin, X. Liu, B. Li, W. Zhang, Y. Yi, M. Zhang, Y. Fu, M. Li, M. Long, Improving the Fenton-like catalytic performance of MnO_x-Fe_3O_4/biochar using reducing agents: a comparative study, J. Hazard. Mater. 406 (2021), 124333, https://doi.org/10.1016/j.jhazmat.2020.124333.

[81] C.J. Miller, Y. Chang, C. Wegeberg, C.J. McKenzie, T.D. Waite, Kinetic analysis of H_2O_2 activation by an iron(III) complex in water reveals a nonhomolytic generation pathway to an iron(IV)oxo complex, ACS Catal. 11 (2) (2021) 787–799, https://doi.org/10.1021/acscatal.0c02877.

[82] K. Chen, L. Que, Stereospecific alkane hydroxylation by non-heme iron catalysts: mechanistic evidence for an $Fe^{V}O$ active species, J. Am. Chem. Soc. 123 (26) (2001) 6327–6337, https://doi.org/10.1021/ja010310x.

[83] S. Kal, S. Xu, L. Que Jr, Bio-inspired nonheme iron oxidation catalysis: involvement of oxoiron(V) oxidants in cleaving strong C-H bonds, Angew. Chem. Int. Edit. 59 (19) (2020) 7332–7349, https://doi.org/10.1002/anie.201906551.

[84] W.N. Oloo, A.J. Fielding, L. Que, Rate-determining water-assisted O-O bond cleavage of an Fe^{III}-OOH intermediate in a bio-inspired nonheme iron-catalyzed oxidation, J. Am. Chem. Soc. 135 (17) (2013) 6438–6441, https://doi.org/10.1021/ja402759c.

[85] R. Mas-Ballesté, L. Que, Iron-catalyzed olefin epoxidation in the presence of acetic acid: Insights into the nature of the metal-based oxidant, J. Am. Chem. Soc. 129 (51) (2007) 15964–15972, https://doi.org/10.1021/ja075115i.

[86] J. Bao, X. Zhang, B. Fan, J. Zhang, M. Zhou, W. Yang, X. Hu, H. Wang, B. Pan, Y. Xie, Ultrathin spinel-structured nanosheets rich in oxygen deficiencies for enhanced electrocatalytic water oxidation, Angew. Chem. Int. Ed. 54 (25) (2015) 7399–7404, https://doi.org/10.1002/anie.201502226.

[87] S. Guo, H. Wang, W. Yang, H. Fida, L. You, K. Zhou, Scalable synthesis of Ca-doped α-Fe_2O_3 with abundant oxygen vacancies for enhanced degradation of organic pollutants through peroxymonosulfate activation, Appl. Catal. B: Environ. 262 (2020), 118250, https://doi.org/10.1016/j.apcatb.2019.118250.

[88] H. Jin, X. Tian, Y. Nie, Z. Zhou, C. Yang, Y. Li, L. Lu, Oxygen vacancy promoted heterogeneous Fenton-like degradation of ofloxacin at pH 3.2-9.0 by Cu substituted magnetic Fe_3O_4@FeOOH nanocomposite, Environ. Sci. Technol. 51 (21) (2017) 12699–12706, https://doi.org/10.1021/acs.est.7b04503.

[89] N. Zhang, E.P. Tsang, J. Chen, Z. Fang, D. Zhao, Critical role of oxygen vacancies in heterogeneous Fenton oxidation over ceria-based catalysts, J. Colloid Interf. Sci. 558 (2020) 163–172, https://doi.org/10.1016/j.jcis.2019.09.079.

[90] H. Li, J. Shang, Z. Yang, W. Shen, Z. Ai, L. Zhang, Oxygen vacancy associated surface Fenton chemistry: surface structure dependent hydroxyl radicals generation and substrate dependent reactivity, Environ. Sci. Technol. 51 (10) (2017) 5685–5694, https://doi.org/10.1021/acs.est.7b00040.

[91] J. Li, J. Miao, X. Duan, J. Dai, Q. Liu, S. Wang, W. Zhou, Z. Shao, Fine-tuning surface properties of perovskites via nanocompositing with inert oxide toward developing superior catalysts for advanced oxidation, Adv. Funct. Mater. 28 (44) (2018) 1804654, https://doi.org/10.1002/adfm.201804654.

[92] X. An, Q. Tang, H. Lan, H. Liu, J. Qu, Polyoxometalates/TiO_2 Fenton-like photocatalysts with rearranged oxygen vacancies for enhanced synergetic degradation, Appl. Catal. B: Environ. 244 (2019) 407–413, https://doi.org/10.1016/j.apcatb.2018.11.063.

[93] H. Li, J. Shang, H. Zhu, Z. Yang, Z. Ai, L. Zhang, Oxygen vacancy structure associated photocatalytic water oxidation of BiOCl, ACS Catal. 6 (12) (2016) 8276–8285, https://doi.org/10.1021/acscatal.6b02613.

[94] K. Zhu, F. Shi, X. Zhu, W. Yang, The roles of oxygen vacancies in electrocatalytic oxygen evolution reaction, Nano Energy 73 (2020), 104761, https://doi.org/10.1016/j.nanoen.2020.104761.

[95] C. Mao, H. Cheng, H. Tian, H. Li, W.-J. Xiao, H. Xu, J. Zhao, L. Zhang, Visible light driven selective oxidation of amines to imines with BiOCl: does oxygen vacancy concentration matter? Appl. Catal. B: Environ. 228 (2018) 87–96, https://doi.org/10.1016/j.apcatb.2018.01.018.

[96] L. Lyu, D. Yan, G. Yu, W. Cao, C. Hu, Efficient destruction of pollutants in water by a dual-reaction-center Fenton-like process over carbon nitride compounds-complexed Cu(II)-$CuAlO_2$, Environ. Sci. Technol. 52 (7) (2018) 4294–4304, https://doi.org/10.1021/acs.est.7b06545.

[97] L. Lyu, L. Zhang, G. He, H. He, C. Hu, Selective H_2O_2 conversion to hydroxyl radicals in the electron-rich area of hydroxylated C-g-C_3N_4/CuCo-Al_2O_3, J. Mater. Chem. A 5 (15) (2017) 7153–7164, https://doi.org/10.1039/C7TA01583F.

[98] L. Lyu, L. Zhang, C. Hu, Galvanic-like cells produced by negative charge nonuniformity of lattice oxygen on d-TiCuAl-SiO_2 nanospheres for enhancement of Fenton-catalytic efficiency, Environ. Sci. Nano 3 (6) (2016) 1483–1492, https://doi.org/10.1039/C6EN00290K.

[99] X. Zhang, Z. Yao, Y. Zhou, Z. Zhang, G. Lu, Z. Jiang, Theoretical guidance for the construction of electron-rich reaction microcenters on C-O-Fe bridges for enhanced Fenton-like degradation of tetracycline hydrochloride, Chem. Eng. J. 411 (2021), 128535, https://doi.org/10.1016/j.cej.2021.128535.

[100] H. Liang, R. Liu, C. Hu, X. An, X. Zhang, H. Liu, J. Qu, Synergistic effect of dual sites on bimetal-organic frameworks for highly efficient peroxide activation, J. Hazard. Mater. 406 (2021), 124692, https://doi.org/10.1016/j.jhazmat.2020.124692.

[101] Y. Zhuang, X. Wang, Q. Liu, B. Shi, N-doped FeOOH/RGO hydrogels with a dual-reaction-center for enhanced catalytic removal of organic pollutants, Chem. Eng. J. 379 (2020), 122310, https://doi.org/10.1016/j.cej.2019.122310.

[102] Y. Zhuang, X. Wang, L. Zhang, D.D. Dionysiou, B. Shi, Fe-Chelated polymer templated graphene aerogel with enhanced Fenton-like efficiency for water treatment, Environ. Sci. Nano 6 (11) (2019) 3232–3241, https://doi.org/10.1039/C9EN00924H.

[103] T. Gao, C. Lu, C. Hu, L. Lyu, H_2O_2 inducing dissolved oxygen activation and electron donation of pollutants over Fe-ZnS quantum dots through surface electron-poor/rich microregion construction for water treatment, J. Hazard. Mater. 420 (2021), 126579, https://doi.org/10.1016/j.jhazmat.2021.126579.

[104] J. Xie, C. Zhang, T.D. Waite, Hydroxyl radicals in anodic oxidation systems: generation, identification and quantification, Water Res. 217 (2022), 118425, https://doi.org/10.1016/j.watres.2022.118425.

[105] Z. Wang, W. Qiu, S.-Y. Pang, Q. Guo, C. Guan, J. Jiang, Aqueous iron(IV)-oxo complex: an emerging powerful reactive oxidant formed by iron(II)-based advanced oxidation processes for oxidative water treatment, Environ. Sci. Technol. 56 (3) (2022) 1492–1509, https://doi.org/10.1021/acs.est.1c04530.

[106] Y. Wen, J. Yan, B. Yang, Z. Zhuang, Y. Yu, Reactive oxygen species on transition metal-based catalysts for sustainable environmental applications, J. Mater. Chem. A 10 (37) (2022) 19184–19210, https://doi.org/10.1039/D2TA02188A.

[107] Y. Chen, C.J. Miller, T.D. Waite, Heterogeneous Fenton chemistry revisited: mechanistic insights from ferrihydrite-mediated oxidation of formate and oxalate, Environ. Sci. Technol. 55 (2021) 14414–14425, https://doi.org/10.1021/acs.est.1c00284.

[108] Y. Nosaka, A. Nosaka, Understanding hydroxyl radical (•OH) generation processes in photocatalysis, ACS Energy Lett. 1 (2) (2016) 356–359, https://doi.org/10.1021/acsenergylett.6b00174.

[109] Y. Wang, L. Chen, C. Chen, J. Xi, H. Cao, X. Duan, Y. Xie, W. Song, S. Wang, Occurrence of both hydroxyl radical and surface oxidation pathways in N-doped layered nanocarbons for aqueous catalytic ozonation, Appl. Catal. B: Environ. 254 (2019) 283–291, https://doi.org/10.1016/j.apcatb.2019.05.008.

[110] L. Xu, J. Wang, Magnetic nanoscaled Fe_3O_4/CeO_2 composite as an efficient Fenton-like heterogeneous catalyst for degradation of 4-chlorophenol, Environ. Sci. Technol. 46 (18) (2012) 10145–10153, https://doi.org/10.1021/es300303f.

[111] G. Yu, Y. Wang, H. Cao, H. Zhao, Y. Xie, Reactive oxygen species and catalytic active sites in heterogeneous catalytic ozonation for water purification, Environ. Sci. Technol. 54 (10) (2020) 5931–5946, https://doi.org/10.1021/acs.est.0c00575.

[112] C. Ling, X. Liu, M. Li, X. Wang, Y. Shi, J. Qi, J. Zhao, L. Zhang, Sulphur vacancy derived anaerobic hydroxyl radical generation at the pyrite-water interface: pollutants removal and pyrite self-oxidation behavior, Appl. Catal. B: Environ. 290 (2021), 120051, https://doi.org/10.1016/j.apcatb.2021.120051.

[113] M. Hayyan, M.A. Hashim, I.M. AlNashef, Superoxide ion: generation and chemical implications, Chem. Rev. 116 (5) (2016) 3029–3085, https://doi.org/10.1021/acs.chemrev.5b00407.

[114] Y. Guo, J. Zhan, G. Yu, Y. Wang, Evaluation of the concentration and contribution of superoxide radical for micropollutant abatement during ozonation, Water Res. 194 (2021), 116927, https://doi.org/10.1016/j.watres.2021.116927.

[115] Y. Guo, Y. Zhang, G. Yu, Y. Wang, Revisiting the role of reactive oxygen species for pollutant abatement during catalytic ozonation: the probe approach versus the scavenger approach, Appl. Catal. B: Environ. 280 (2021), 119418, https://doi.org/10.1016/j.apcatb.2020.119418.

[116] S.M. Mitchell, M. Ahmad, A.L. Teel, R.J. Watts, Degradation of perfluorooctanoic acid by reactive species generated through catalyzed H_2O_2 propagation reactions, Environ. Sci. Tech. Let. 1 (1) (2014) 117–121, https://doi.org/10.1021/ez4000862.

[117] C.K.O. da, Silva-Rackov, W.A. Lawal, P.A. Nfodzo, M.M.G.R. Vianna, C.A.O. do Nascimento, H. Choi, Degradation of PFOA by hydrogen peroxide and persulfate activated by iron-modified diatomite, Appl. Catal. B: Environ. 192 (2016) 253–259, https://doi.org/10.1016/j.apcatb.2016.03.067.

[118] H. Javed, J. Metz, T.C. Eraslan, J. Mathieu, B. Wang, G. Wu, A.-L. Tsai, M. S. Wong, P.J.J. Alvarez, Discerning the relevance of superoxide in PFOA degradation, Environ. Sci. Technol. Lett. 7 (9) (2020) 653–658, https://doi.org/10.1021/acs.estlett.0c00505.

[119] O. Furman, D.F. Laine, A. Blumenfeld, A.L. Teel, K. Shimizu, I.F. Cheng, R. J. Watts, Enhanced reactivity of superoxide in water-solid matrices, Environ. Sci. Technol. 43 (5) (2009) 1528–1533, https://doi.org/10.1021/es802505s.

[120] L. Li, M. Cheng, L. Qin, E. Almatrafi, X. Yang, L. Yang, C. Tang, S. Liu, H. Yi, M. Zhang, Y. Fu, X. Zhou, F. Xu, G. Zeng, C. Lai, Enhancing hydrogen peroxide activation of CuCo layered double hydroxide by compositing with biochar: performance and mechanism, Sci. Total Environ. 828 (2022), 154188, https://doi.org/10.1016/j.scitotenv.2022.154188.

[121] Z. Yang, J. Qian, A. Yu, B. Pan, Singlet oxygen mediated iron-based Fenton-like catalysis under nanoconfinement, Proc. Natl. Acad. Sci. 116 (14) (2019) 6659, https://doi.org/10.1073/pnas.1819382116.

[122] M. Zhou, J. Chen, S. Yu, B. Chen, C. Chen, L. Shen, B. Li, H. Lin, The coupling of persulfate activation and membrane separation for the effective pollutant degradation and membrane fouling alleviation, Chem. Eng. J. 451 (2023), 139009, https://doi.org/10.1016/j.cej.2022.139009.

[123] J. Al-Nu'airat, I. Oluwoye, N. Zeinali, M. Altarawneh, B.Z. Dlugogorski, Review of chemical reactivity of singlet oxygen with organic fuels and contaminants, Chem. Rec. 21 (2) (2021) 315–342, https://doi.org/10.1002/tcr.202000143.

[124] A.D. Bokare, W. Choi, Singlet-oxygen generation in alkaline periodate solution, Environ. Sci. Technol. 49 (24) (2015) 14392–14400, https://doi.org/10.1021/acs.est.5b04119.

[125] C. Yuan, M. Chakraborty, S. Canonica, L.K. Weavers, C.M. Hadad, Y.-P. Chin, Isoproturon reappearance after photosensitized degradation in the presence of triplet ketones or fulvic acids, Environ. Sci. Technol. 50 (22) (2016) 12250–12257, https://doi.org/10.1021/acs.est.6b03655.

[126] L. Pan, W. Shi, T. Sen, L. Wang, J. Zhang, Visible light-driven selective organic degradation by $FeTiO_3$/persulfate system: the formation and effect of high valent Fe(IV), Appl. Catal. B: Environ. 280 (2021), 119414, https://doi.org/10.1016/j.apcatb.2020.119414.

[127] D.O. Mártire, P. Caregnato, J. Furlong, P. Allegretti, M.C. Gonzalez, Kinetic study of the reactions of oxoiron(IV) with aromatic substrates in aqueous solutions, Int. J. Chem. Kinet. 34 (8) (2002) 488–494, https://doi.org/10.1002/kin.10076.

[128] O. Pestovsky, A. Bakac, Reactivity of aqueous Fe(IV) in hydride and hydrogen atom transfer reactions, J. Am. Chem. Soc. 126 (42) (2004) 13757–13764, https://doi.org/10.1021/ja0457112.

[129] Z. Wang, W. Qiu, S. Pang, J. Jiang, Effect of chelators on the production and nature of the reactive intermediates formed in Fe(II) activated peroxydisulfate and hydrogen peroxide processes, Water Res. 164 (2019), 114957, https://doi.org/10.1016/j.watres.2019.114957.

[130] H. Li, C. Shan, B. Pan, Fe(III)-doped g-C_3N_4 mediated peroxymonosulfate activation for selective degradation of phenolic compounds via high-valent iron-oxo species, Environ. Sci. Technol. 52 (4) (2018) 2197–2205, https://doi.org/10.1021/acs.est.7b05563.

[131] Z.-J. Dong, C.-C. Jiang, Q. Guo, J.-W. Li, X.-X. Wang, Z. Wang, J. Jiang, A novel diagnostic method for distinguishing between Fe(IV) and •OH by using atrazine as a probe: clarifying the nature of reactive intermediates formed by nitrilotriacetic acid assisted Fenton-like reaction, J. Hazard. Mater. 417 (2021), 126030, https://doi.org/10.1016/j.jhazmat.2021.126030.

[132] H. Bataineh, O. Pestovsky, A. Bakac, Electron transfer reactivity of the aqueous iron(IV)-oxo complex. Outer-sphere vs proton-coupled electron transfer, Inorg. Chem. 55 (13) (2016) 6719–6724, https://doi.org/10.1021/acs.inorgchem.6b00966.

[133] H. Zhao, J. Gao, W. Zhou, Z. Wang, S. Wu, Quantitative detection of hydroxyl radicals in Fenton system by UV-vis spectrophotometry, Anal. Methods 7 (13) (2015) 5447–5453, https://doi.org/10.1039/C5AY00514K.

[134] W. Yu, L. Zhao, Chemiluminescence detection of reactive oxygen species generation and potential environmental applications, TrAC Trend. Anal. Chem. 136 (2021), 116197, https://doi.org/10.1016/j.trac.2021.116197.

[135] J. Du, C. Wang, Z. Zhao, F. Cui, Q. Ou, J. Liu, Role of oxygen and superoxide radicals in promoting H_2O_2 production during VUV/UV radiation of water, Chem. Eng. Sci. 241 (2021), 116683, https://doi.org/10.1016/j.ces.2021.116683.

[136] L. Wang, B. Li, D.D. Dionysiou, B. Chen, J. Yang, J. Li, Overlooked formation of H_2O_2 during the hydroxyl radical-scavenging process when using alcohols as scavengers, Environ. Sci. Technol. 56 (6) (2022) 3386–3396, https://doi.org/10.1021/acs.est.1c03796.

[137] L. Gao, Y. Guo, J. Zhan, G. Yu, Y. Wang, Assessment of the validity of the quenching method for evaluating the role of reactive species in pollutant abatement during the persulfate-based process, Water Res. 221 (2022), 118730, https://doi.org/10.1016/j.watres.2022.118730.

[138] Y. Guo, J. Long, J. Huang, G. Yu, Y. Wang, Can the commonly used quenching method really evaluate the role of reactive oxygen species in pollutant abatement during catalytic ozonation? Water Res. 215 (2022), 118275 https://doi.org/10.1016/j.watres.2022.118275.

[139] Y. Nakabayashi, Y. Nosaka, OH radical formation at distinct faces of rutile TiO_2 crystal in the procedure of photoelectrochemical water oxidation, J. Phys. Chem. C 117 (45) (2013) 23832–23839, https://doi.org/10.1021/jp408244h.

[140] J.-F. Jen, M.-F. Leu, T.C. Yang, Determination of hydroxyl radicals in an advanced oxidation process with salicylic acid trapping and liquid chromatography, J. Chromatogr. A 796 (2) (1998) 283–288, https://doi.org/10.1016/S0021-9673(97)01019-4.

[141] N. Chen, Y. Huang, X. Hou, Z. Ai, L. Zhang, Photochemistry of hydrochar: reactive oxygen species generation and sulfadimidine degradation, Environ. Sci. Technol. 51 (19) (2017) 11278–11287, https://doi.org/10.1021/acs.est.7b02740.

[142] J. Wang, L. Liu, W. Xu, Z. Yang, Y. Yan, X. Xie, Y. Wang, T. Yi, C. Wang, J. Hua, Mitochondria-targeted ratiometric fluorescent probe based on diketopyrrolopyrrole for detecting and imaging of endogenous superoxide anion in vitro and in vivo, Anal. Chem. 91 (9) (2019) 5786–5793, https://doi.org/10.1021/acs.analchem.9b00014.

[143] Y. Kakuma, A.Y. Nosaka, Y. Nosaka, Difference in TiO_2 photocatalytic mechanism between rutile and anatase studied by the detection of active oxygen and surface species in water, Phys. Chem. Chem. Phys. 17 (28) (2015) 18691–18698, https://doi.org/10.1039/C5CP02004B.

[144] H. Wu, Q. Song, G. Ran, X. Lu, B. Xu, Recent developments in the detection of singlet oxygen with molecular spectroscopic methods, TrAC Trend. Anal. Chem. 30 (1) (2011) 133–141, https://doi.org/10.1016/j.trac.2010.08.009.

[145] K. Tanaka, T. Miura, N. Umezawa, Y. Urano, K. Kikuchi, T. Higuchi, T. Nagano, Rational design of fluorescein-based fluorescence probes. Mechanism-based design of a maximum fluorescence probe for singlet oxygen, J. Am. Chem. Soc. 123 (11) (2001) 2530–2536, https://doi.org/10.1021/ja0035708.

[146] N. Soh, Recent advances in fluorescent probes for the detection of reactive oxygen species, Anal. Bioanal. Chem. 386 (3) (2006) 532–543, https://doi.org/10.1007/s00216-006-0366-9.

[147] J. Ma, W. Lv, P. Chen, Y. Lu, F. Wang, F. Li, K. Yao, G. Liu, Photodegradation of gemfibrozil in aqueous solution under UV irradiation: kinetics, mechanism, toxicity, and degradation pathways, Environ. Sci. Pollut. R. 23 (14) (2016) 14294–14306, https://doi.org/10.1007/s11356-016-6451-5.

[148] M.M. Rodrigues, I.M.B. Francischetti, E. Gordon, B. Bizzarro, N. Gera, B. B. Andrade, F. Oliveira, D. Ma, T.C.F. Assumpção, J.M.C. Ribeiro, M. Pena, C.-F. Qi, A. Diouf, S.E. Moretz, C.A. Long, H.C. Ackerman, S.K. Pierce, A. Sá-Nunes, M. Waisberg, Tempol, an intracellular antioxidant, inhibits tissue factor expression, attenuates dendritic cell function, and is partially protective in a murine model of cerebral malaria, PLoS One 9 (2) (2014) 87140, https://doi.org/10.1371/journal.pone.0087140.

[149] Y. Zong, Y. Mao, L. Xu, D. Wu, Non-selective degradation of organic pollutants via dioxygen activation induced by Fe(II)-tetrapolyphosphate complexes: identification of reactive oxidant and kinetic modeling, Chem. Eng. J. 398 (2020), 125603, https://doi.org/10.1016/j.cej.2020.125603.

[150] Y. Zhou, J. Jiang, Y. Gao, J. Ma, S.-Y. Pang, J. Li, X.-T. Lu, L.-P. Yuan, Activation of peroxymonosulfate by benzoquinone: a novel nonradical oxidation process, Environ. Sci. Technol. 49 (21) (2015) 12941–12950, https://doi.org/10.1021/acs.est.5b03595.